Experimental Analysis of Surface Finish in Normal Conducting Cavities

A. Zarrebini-Esfahani[1], M. Aslaninejad[2], M. Ristic[1], K. Long[3]

[1]*Imperial College London,* Department of Mechanical Engineering, London, UK

[2]*School of Particles and Accelerators, Institute for Research in Fundamental Sciences (IPM), P.O. Box 19395-5531, Tehran, Iran*

[3]*Imperial College London,* Blackett Lab, High Energy Physics Department, London, UK

Abstract

A normal conducting 805 MHz test cavity with an in built button shaped sample is used to conduct a series of surface treatment experiments. The button enhances the local fields and influences the likelihood of an RF breakdown event. Because of their smaller sizes, compared to the whole cavity surface, they allow practical investigations of the effects of cavity surface preparation in relation to RF breakdown. Manufacturing techniques and steps for preparing the buttons to improve the surface quality are described in detail. It was observed that even after the final stage of the surface treatment, defects on the surface of the cavities still could be found.

I. INTRODUCTION

In a Neutrino Factory complex pions are created by bombarding a target by protons and are captured by a magnetic field at low energy where they decay to muons [1-2]. The phase space of the muons is controlled and shrunk through bunching and cooling. They would be accelerated later and injected into storage rings with long straight sections where muons decay to produce neutrinos that are directed towards the detectors [1-2].

The reduction in the transverse emittance of muons is achieved through a technique known as ionisation cooling where muon beam is cooled through energy loss at absorbers [3-5]. Existing techniques such as stochastic, electron and laser cooling for transverse emittance reduction are not feasible due to the muon's short lifetime of 2.2 μs [4]. The net effect of transverse cooling can be achieved if the longitudinal momentum is restored through re-acceleration. The Muon Ionisation Cooling Experiment (MICE) is essentially a proof of this principle and is based at the Rutherford Appleton Laboratory (RAL) [3-7]. The MICE experiment consists of a cooling section positioned between a pair of particle spectrometers. The 200 MeV muon beam is generated from the ISIS 800 MeV proton beam at Rutherford Appleton Laboratory (RAL). The cooling cell is made out of two 201 MHz cavities, one primary and two secondary LiH absorbers placed between two superconducting focusing coil modules. The cooling cell is also sandwiched between two spectrometer solenoid modules [5].

The MuCool Test Area (MTA) is a dedicated facility built at Fermilab [6] to support the technology development for muon ionization cooling channels. The main purpose is to assess the characteristics of an RF cavity under the same conditions as those experienced in an ionisation cooling channel. The principal components at the MTA are the 201 MHz MICE test cavity and a higher frequency (and smaller size) 805 MHz button test cavity. The 805 MHz test cavity is positioned inside a 4 Tesla (T) superconducting solenoid, and closely resembles a cylindrical pillbox cavity with Beryllium windows covering the irises. The experiment has been designed to allow for demountable windows to be installed. As a result, various physics are being investigated through different tests, such as those involving button samples. The cavity parameters are given in Table. 1.

Table.1: Main MTA 805 MHz cavity parameters

Parameter	**Value**	**Unit**
Frequency	805	MHz
Cavity radius	15.62	cm
Gap length	8.1	cm
Be windows thickness	0.127	mm
Cavity shunt Impedance	32	MΩ/m
Cavity quality factor Q	18800	

A major goal of the MTA program is to test and investigate the performance of different materials and surface treatments in the presence of high electric and magnetic fields. The prime interest is the manufacture of 201 MHz, which demands sheet metal processing. The 201 MHz cavities, however, do not accommodate button samples. The 805 MHz cavities are small enough to be manufactured by machining from solid bulk and accommodate button samples. New buttons had to be designed, which could be manufactured using sheet metal techniques and tested in the 805 MHz cavity. The button shape enhances the field locally, ensuring any possible breakdown occurring on the button surface. The performance of the sample is analysed by increasing the field strength in steps until RF breakdown has occurs. The buttons allow for a wide variety of materials to be tested with quick and easy changeover between the samples. They also provide a practical way to use small samples instead of the whole cavities for the purpose of testing the cavity surface preparation. This forms the basis for the surface roughness measurement experiment, where button samples are produced and treated using a series of manufacturing and preparation techniques. RF breakdown with external magnetic field in 201 MHz and 805 MHz cavities were studied at the MTA [10]. The MTA group has investigated the field emission characteristics of various materials and the effects of an externally applied magnetic field on such emissions [8,9]. The quality of the RF surface has been identified as a major factor contributing to RF breakdown [10]. Hence this research has focused on the quality of the RF surface and how various production and surface treatment techniques alter the final surface finish. A new button testing program was defined focusing on manufacturing techniques instead of material. While the button design was changed, the overall size and shape was kept similar to the MTA button. This was to allow complete compatibility with the testing equipment available at the MTA testing area.

The structure of the paper is as follows. Sec. II introduces fabrication setup used to manufacture each button sample. This is followed by the introduction of the processing setup used to treat the surface of each button in Sec. III. The main methods employed for the surface treatment are hand polishing, chemical etching, electro polishing (EP) and electro plating (EPL). A

detailed investigation in to the quality of the RF surface is presented in Sec. IV, highlighting the changes observed during various stages of production. Surface roughness [11] for each button is investigated quantitatively in terms of Average and Root Mean Square (RMS) surface roughness. Finally, we summarise our results in the conclusions made in Sec. V.

II. Button Fabrication Techniques

During the production of an RF cavity, the metallic surface experiences both mechanical and chemical alterations. Hence the quality of the RF surface is directly influenced by the manufacturing techniques employed during production. The quality of the RF surface can influence the probability of an RF breakdown event.

In order to enhance the performance of the cavity, production methods need to be improved and further investigated. The MTA research program has been performing a series of high power tests on button shaped samples using an 805 MHz copper cavity. The aim is to investigate the RF breakdown limit of various materials by exposing each to high E and B fields [12-18]. Our focus, however, is on the manufacturing techniques rather than material properties of the buttons [19-21].

The new design of the button test piece is shown in left panel of the Fig. 1. Although the overall shape is similar to the MTA design (Fig. 1 far left), the new design consists of two separate detachable parts. The upper part known as the cap is subject to RF fields inside the cavity and is held in the correct position by the holder. A major benefit of such a design is the ability to use a wider range of fabrication techniques due to simpler design. During testing, the cap and holder need to stay as one unit. This was achieved by drilling six equally spaced holes in the holder, each housing a ball bearing and spring mechanism. When in position, the springs generate the necessary friction between the cap and the holder by pushing the ball bearings towards the internal walls of the cap. A series of air vents are incorporated in the holder to ensure no air pockets are trapped when operating in vacuum.

To replicate the processes used for the production of the MICE 201 MHz cavity, sheet metal drawing was used as the fabrication method. The cap is made out of a 1 mm thick copper sheet. As shown in Fig. 1 (right), the cap was pressed in four different stages, achieving the final shape. The staged deformation process was designed to avoid possible rupture when stretching the material. The material of choice for normal conducting cavities is Oxygen-Free High

Conductivity (OFHC) copper. This generally refers to a group of wrought, high conductivity a copper that has been refined to reduce oxygen levels.

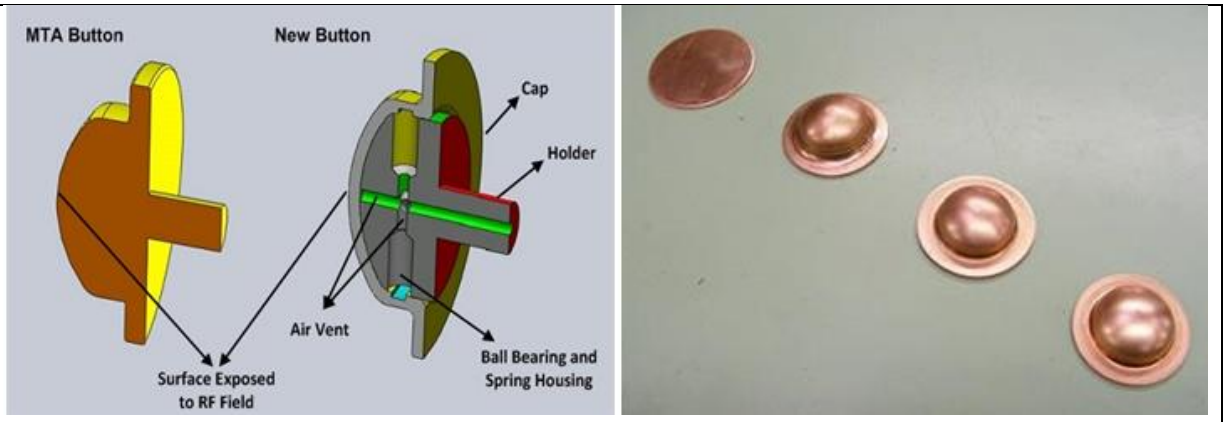

Fig. 1: Cross sectional view of the current MTA button (far left) and new design (left); four stages of Cap piece fabrication (right)

The cap was manufactured using OFHC to match the characteristics of MICE and MTA cavities. The oxygen purity level of the OFHC used in this research was 99.99% [22]. The holder on the other hand, is not subject to RF fields but needs to be operated in the presence of high magnetic fields. To fulfil such requirement, the holder was made out of aluminium alloy with high mechanical strength and ability for easy machining. Furthermore, attention was paid to choose austenite stainless steel for each ball bearing and spring mechanism.

Optical profiling measurement system was used to take the necessary surface roughness measurements. The apparatus used is WYKO NT1100, which is a 3D optical profiling measurement system. The scanning measurement area is 736 by 480 microns. In order to provide a better characterisation of the surface of each sample, measurements were taken at various locations. A total of 16 data points on 4 concentric circles were chosen for the purpose of measurement. As shown in Fig. 2, the apex is counted four times. The overall surface roughness parameters were derived by averaging the roughness of the all sixteen data points. To preserve the accuracy of measurements the incident light was kept orthogonal to the cap surface. This was achieved by designing and manufacturing a scanning holder tool.

The RF surface was prepared using different surface treatment methods. An X-ray Photoelectron Spectroscopy (XPS) was utilised to analyse the chemical composition of the button samples. By taking measurements after each major stage of production, it was possible to identify the changes of the surface characteristics for each sample.

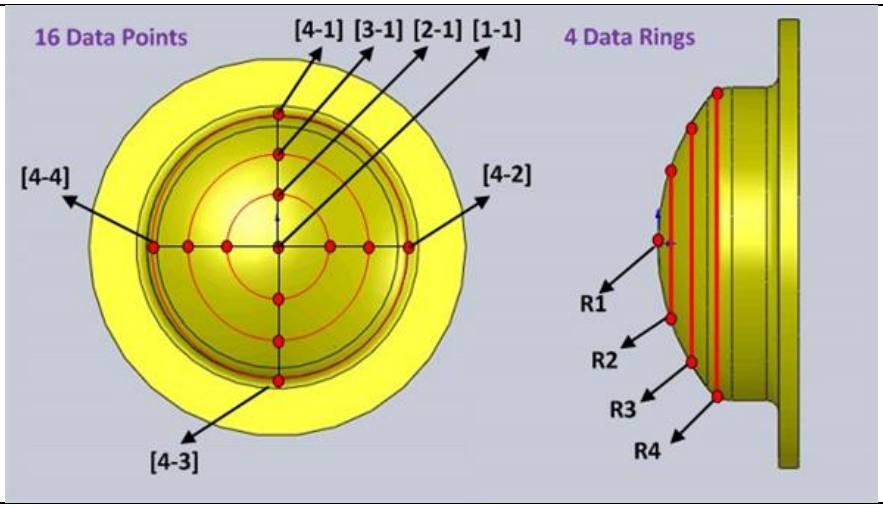

Fig. 2: Representation of the chosen data points and rings for each button Cap

III. Surface Treatment Methods

The quality of the RF surface is of much importance for the overall performance of any accelerating structure. Hence, surface preparation is considered to be the most vital aspect in the production of high gradient RF cavities [2326]. Several buttons were manufactured using the fabrication processes described in the previous section. The surfaces of the buttons in each group were treated using two different methods and comparisons were made.

III-a. Electro-polishing (EP)

Electro polishing (EP) is the most commonly used technique to treat the surfaces of RF cavities including the MICE and the MTA cavities. Hence, EP was chosen as the final stage of the surface treatment method one and was used to polish the buttons B_1 to B_6. Each button underwent a series of stages including, fabrication (A), hand polishing (B), chemical etching (C) and EP (D). This surface quality for button B_1 is shown in Fig.3, where steps A to C were carried out to remove the most contaminated and damaged layers prior to performing EP. The sheet metal pressing technique generally leads to a very poor surface finish. This is due to the nature of the process, where the metallic surface is pressed against a rough forming tool. Furthermore, the surface is easily contaminated by foreign particles such as manufacturing grease and oxide layer. What is immediately evident in Fig. 3 (A), is the damage inflicted on the surface from the pressing process which is typical of the surfaces observed. Hand polishing was performed in a circular motion using sand papers with grades ranging from P120 to P600.

As shown in Fig. 3 (B), deeper cuts were replaced with random arrays of tiny scratches. These tend to follow the movement of the abrasive paper during hand polishing process. However,

process B was capable of removing the damaged layer seen previously due to fabrication procedure. Metallic dust and paper contaminations were removed by washing the button in an ultra-sonic bath. The next step in the surface preparation was chemical etching in which the button was submerged into a bath of phosphoric acid. As shown in Fig.3 (C), button B_1 was chemical etched for two hours and the majority of the sharp edges around surface scratches were removed. No visible patterns were observed due to the random nature of the chemical etching process. It is crucial to perform process C prior to EP in order to achieve a superior final surface finish. This is due to the fact that the virgin copper is ultimately exposed after performing both processes B and C. The quality of the surface generated is evident as there are no visible scratches present on the button surface, resulting in a mirror-like finish.

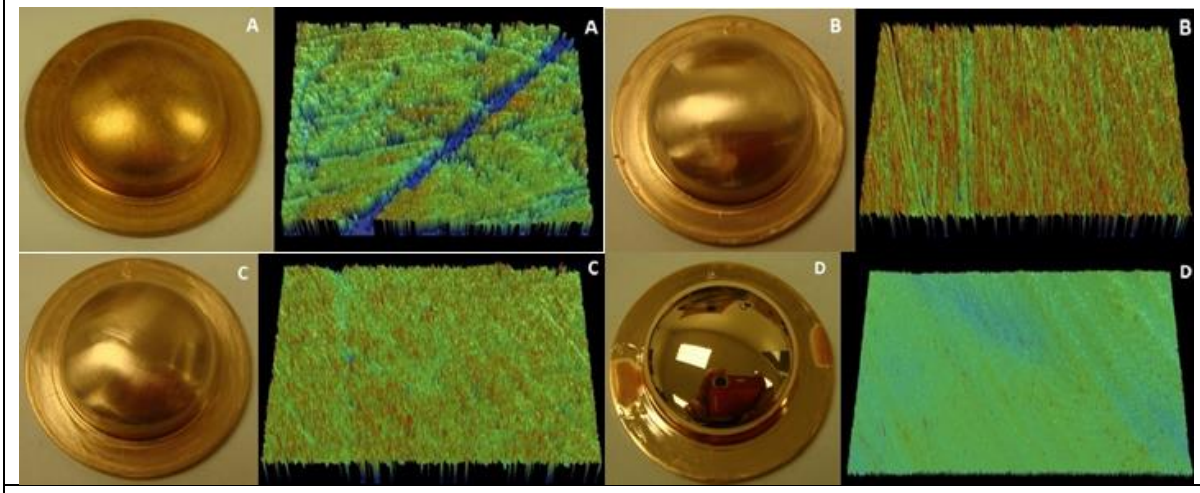

Fig. 3. The surface quality and its 3D plot for button B_1, as received (A), Hand polished (B), Chemically etched (C) and electro polished (D)

Similar to the MTA studies [10, 14] the electrolyte mix was comprised of 85% phosphoric acid and 15% butanol. Fig. 4 shows the EP setups used for the MICE cavity, MTA buttons and the improved setup used in this study. A U-shaped cathode was placed inside the MICE cavity while the acid was slushed around by rotating the cavity [15]. The main drawback of this setup is that the cavity is continually exposed to fresh air and oxidisation as the cavity is rotated around its axis. The MTA buttons were polished using a High Density Polyethylene box filled with acid while both the cathode and anode sat side by side. Although this setup allowed for more than one button to be polished at any time, it was limited by the lack of ability to apply a steady voltage across the surface of the button. Such limitations were addressed in this study by redesigning the EP setup used to polish the new buttons. Once the electric current is applied through the mixture, the conditions of the electrolyte are subject to a continuous change.

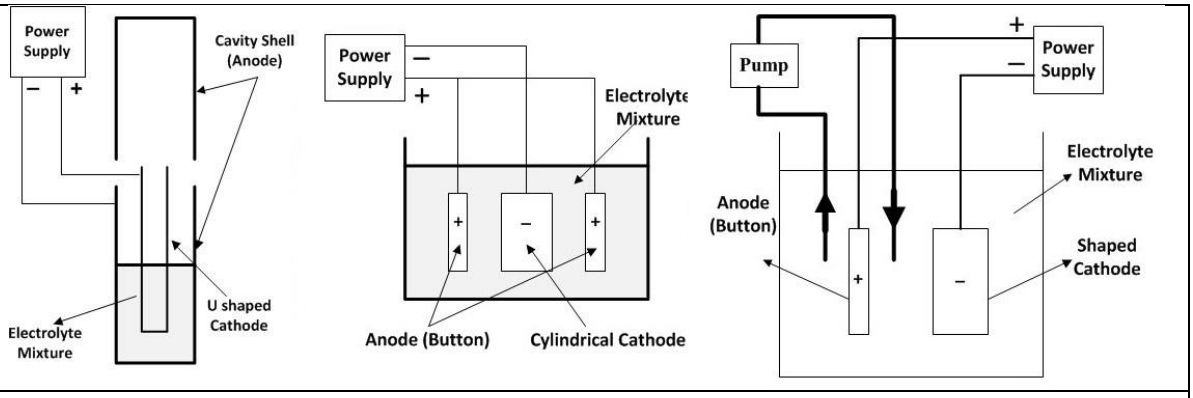

Fig.4. Schematic view of the EP polishing setup used for the MICE 201 MHz cavity (left) MTA buttons (middle) Buttons used in this study (right)

The most noticeable change was the formation of the oxygen bubbles. The conductivity characteristics of the mixture eventually faded away as the mixture turned into a light blue colour. The cathode was shaped as the negative mirror of the button to allow a more even application of current across the surface of the button. The electrolyte was circulated around the anode through an agitation pump to eliminate oxygen build up.

The EP process was initially tried and tested on 9 test samples referred to as samples T_1 to T_9. The aim was to determine the necessary characteristics of a reliable EP setup and to obtain a stable polishing plateau. Each test sample was polished using a changed EP setup and the final outcome was evaluated in order to define the final setup. Fig 5 demonstrates the main changes made for three of the test samples. The desirable distance between the anode and cathode was set at 5 cm. The curved cathode was changed to a flat sheet of copper for T_1, while the agitation pump was removed for T_2 with a curved cathode. Test sample T_3 used the same curved cathode but with twice the distance from the button.

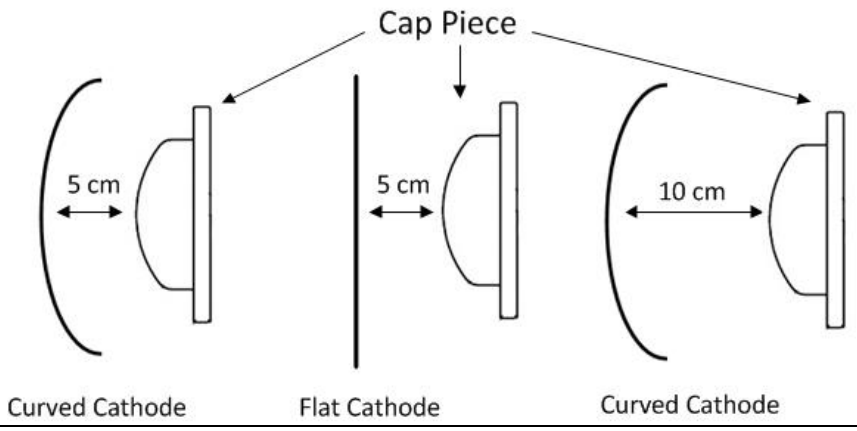

Fig.5 The shape and position of the cathode in relation to the button for test samples T_3 with no agitation (left) T_1 with agitation (middle) T_2 with agitation (right)

The surface quality for test samples T_1, T_2 and T_3 are shown in Fig 6. Changing the cathode to a flat sheet resulted in an uneven current application across the surface of the sample. This was due to the changes in the EP plateau observed during the polishing process, resulting in a poor surface finish. Increasing the distance between the cathode and anode resulted in the reduction of current passing through the electrolyte, leading to a drop in the quality of the surface finish. The removal of the agitation pump for sample T_3 led to the oxygen saturation in the near vicinity of the cathode, hence generating an early peak in the applied current. This significant change in the polishing plateau resulted in a remarkably poor surface finish. The final EP setup to polish all button in this study was similar to of that for T_3 with an adequate level of agitation to ensure the electrolyte was circulated sufficiently.

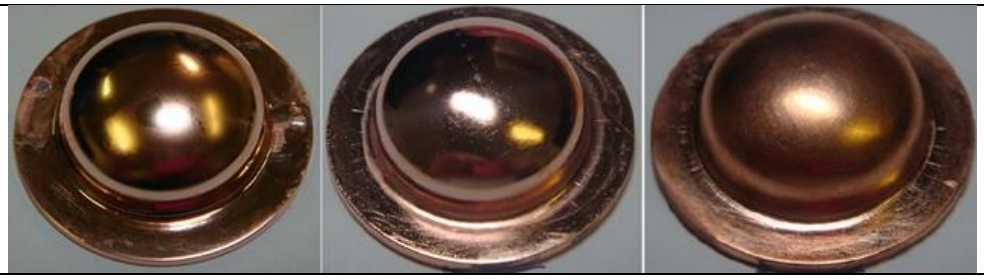

Fig.6 Polished test sample T_1 with a flat cathode (left), sample T_2 with shaped cathode and longer distance to the anode (middle), sample T_3 with similar set up to buttons B_1-B_6 with no agitation pump (right)

It was evident that the changing conditions of the polishing setup had dramatic alterations on the quality of the surface finished during EP. Hence, a standard EP setup was chosen in order to keep the polishing conditions as steady as possible for all the buttons used in this study. The pump speed was set to 50 rpm, ensuring the electrolyte is agitated adequately. The time required to reach the cusp point of the plateau varied based on the mixture behaviour. Once the cusp point voltage was reached, each button was polished for two hours. Buttons B_1, B_3 and B_5 were polished using a fresh mixture of electrolyte. On the other hand, buttons B_2, B_4 and B_6 used an electrolyte mixed that was used once already. The preparation time to reach the optimal current for buttons B_1 and B_4 was 30 minutes, for B_2 and B_5, 20 minutes, for B_3, 25 minutes and for B_6 was 35 minutes. The cusp point voltage for buttons B_1, B_4, B_5 and B_6 was 1.5 V and 1.6 V for B_2 and B_3. The current for all buttons was 0.73 A, except for button B_3 which was 0.83 A. To preserve the electrolyte characteristics, each mixture was only used twice. Fig. 7 shows the polishing plateau and current passing through the electrolyte for samples B_1 to B_6.

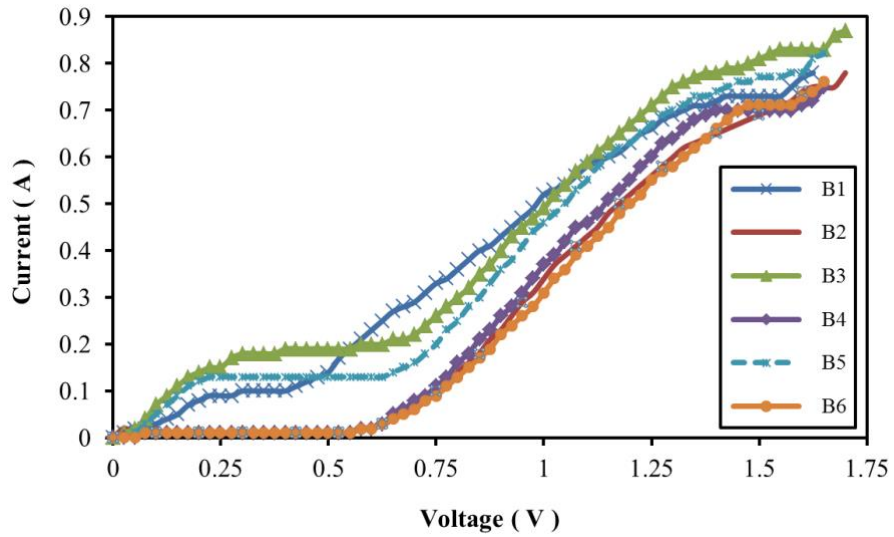

Fig. 7. Current versus voltage behaviour in electro polishing of buttons B_1 to B_6

III-b. Electro-plating (EPL)

While EP was used as the main surface treatment process in method one, this was used as a pre-treatment stage prior to electro plating in method two. EPL is the application of electrolytic cells in which a thin layer of metal is deposited onto an electrically conductive surface. A total of six more buttons numbered B_7 to B_{12} were produced and treated using EPL. All the processes in method one were performed before carrying out the EPL stage. At the end, each button was coated with a fresh layer of OFHC copper. Fig. 8 illustrates the quality of the surface finish achieved after performing EPL on button B_7. Similar to the previous method, a mirror like surface finish was achieved. This was an indication of the quality of the deposited layer and the cohesion made with the underlying electro polished surface.

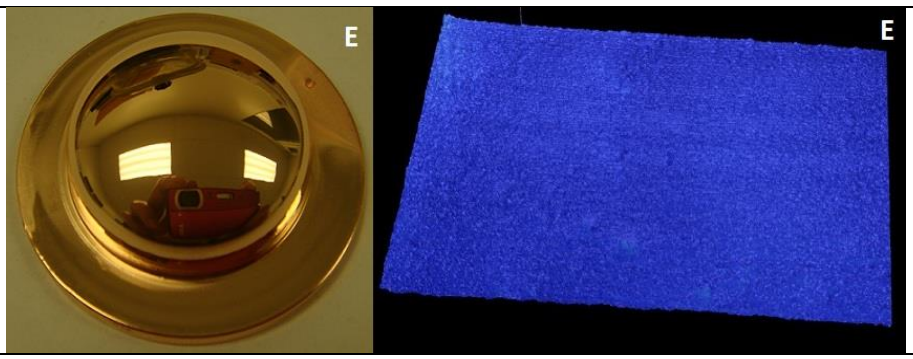

Fig. 8. The surface quality and its 3D plot for button B_7 after electro plating (E)

The rate of deposition is based on the input current passing through the copper bath. This is also directly related to the surface area of the sample being plated. Based on the 15.59 cm^2 surface area of each button, an input current on 0.6 amps is required to deposit 1 μ of coating per minute. Each button was coated for a duration of two hours.

IV. Surface Roughness

The arithmetic average roughness can be expressed as [11]:

$$R_a = \frac{1}{L}\int_0^L |y(x)|dx = \frac{1}{n}\sum_{i=1}^{n}|y_i| \qquad (1)$$

where L is the sampling length, n the total number of samples and y is the surface profile being investigated.

Root mean square (RMS) roughness represents standard deviation of the surface heights distribution. The advantage of this parameter compared to arithmetic average roughness is the sensitivity of this parameter to small deviation from the mean line. The root mean square roughness can be expressed mathematically as [11]:

$$R_q = \sqrt{\frac{1}{n}\int_0^1 \{y(x)\}^2 dx} = \sqrt{\frac{1}{n}\sum_{i=1}^{n} y_i^2} \qquad (2)$$

We also used a non-standard measurement of (R_q-R_a) as a roughness parameter referred to as surface uniformity. It acts as a means to emphasise the differences between the overall peaks and troughs of a surface profile. A higher value of the (Rq-Ra) implies a lower surface uniformity. The R_q parameter can be used to make comparisons between two surfaces with similar Ra values and analyse the overall quality of the surface. The overall roughness measurements for button B1 are shown in Table 2. These are an average of the data recorded for all the data points across the surface of the button after each stage of the treatment process.

Table 2: Average roughness (R_a) and root mean square (R_q) parameters for Button B_1

Process	**A (as received)**	**B (hand polished)**	**C (chemical etch)**	**D (electro polish)**
R_a (nm)	491	279	298	154
R_q (nm)	631	364	415	194

Shown in Fig. 3, it was learned that once the button left the production line the surface quality was at its lowest and was validated based on the surface roughness measurements taken. R_a was gradually reduced throughout the processes apart from a slight rise seen during process C. This was simply due to the nature of the chemical etching and should not be regarded as deterioration in the quality of the surface. Chemical etching was performed to blunt the sharp edges, preparing the surface for EP. This was an uncontrolled process, leading to an increase in average roughness parameters. In addition to R_a, we also employed surface uniformity (R_q-R_a) to further investigate the changes in the surface quality.

Fig. 9 shows the roughness parameters for button B_1, obtained by averaging the measurements from all the data points. The surface quality was improved as the roughness measurements were lowered and uniformity was increased. Note that the vertical bars in Fig. 8 represent the variations in the roughness parameter obtained from all 16 data points and should not be confused as error bars. For instance, the scale of variation between obtained parameters of the process A shows the uncontrolled nature of the production technique used to fabricate the button. By enabling the user to have better control over the outcome of processes B and C, lower variations in surface roughness parameters were observed. The average roughness was reduced further once EP was performed. The small variations seen in roughness measurements during process D, highlights the robust nature of the EP setup.

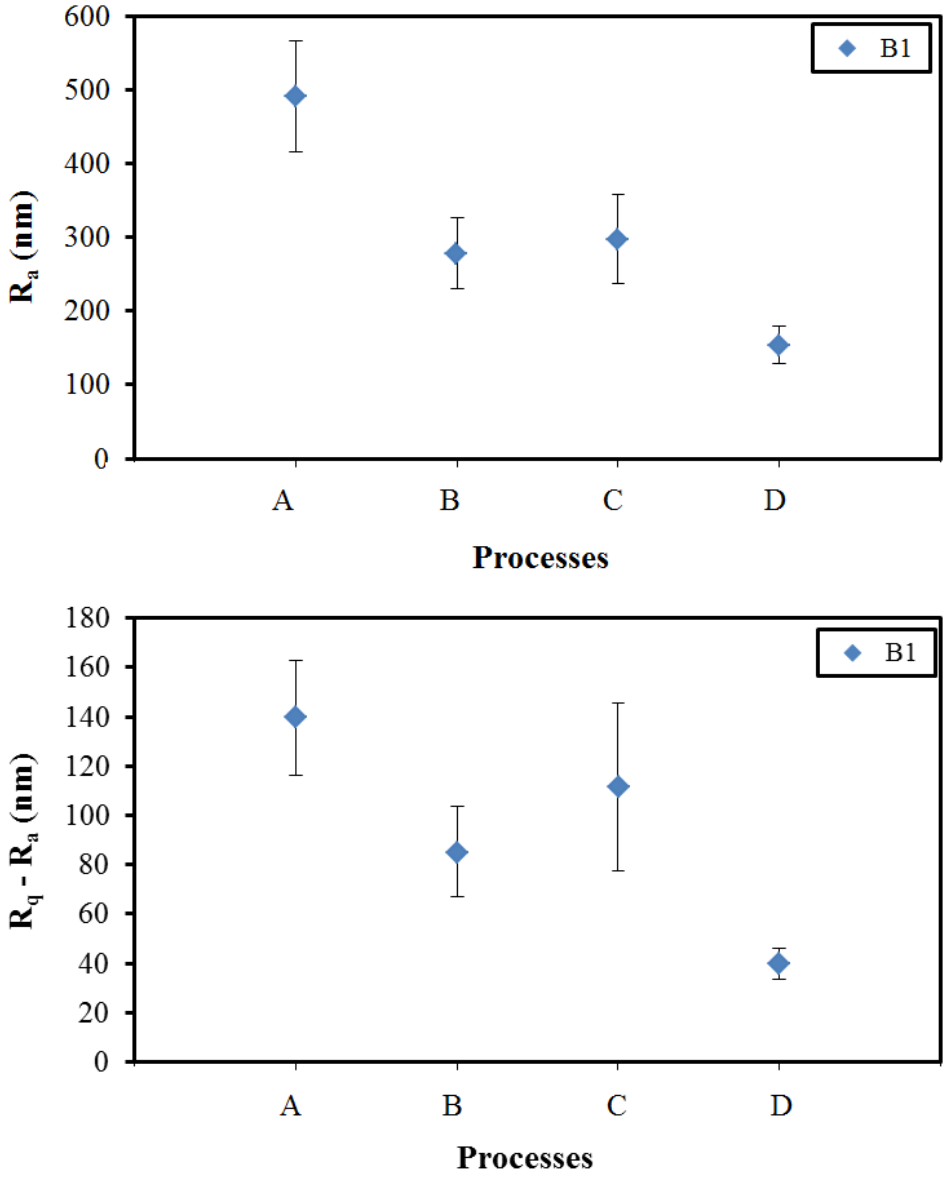

Fig. 9 Surface roughness measurements taken for button B_1, Ra (top); R_q-R_a (bottom)

To provide a more detailed look at the changing surface quality, roughness parameters of data rings should be investigated alongside individual data points. Fig. 10 illustrates the measured parameters of such rings for button B_1 throughout the processes. During fabrication, the outer edges of the button experience a higher level of physical damage due to the increase of mechanical pressure. This is clearly evident in Fig. 10, where R4 showed higher surface roughness.

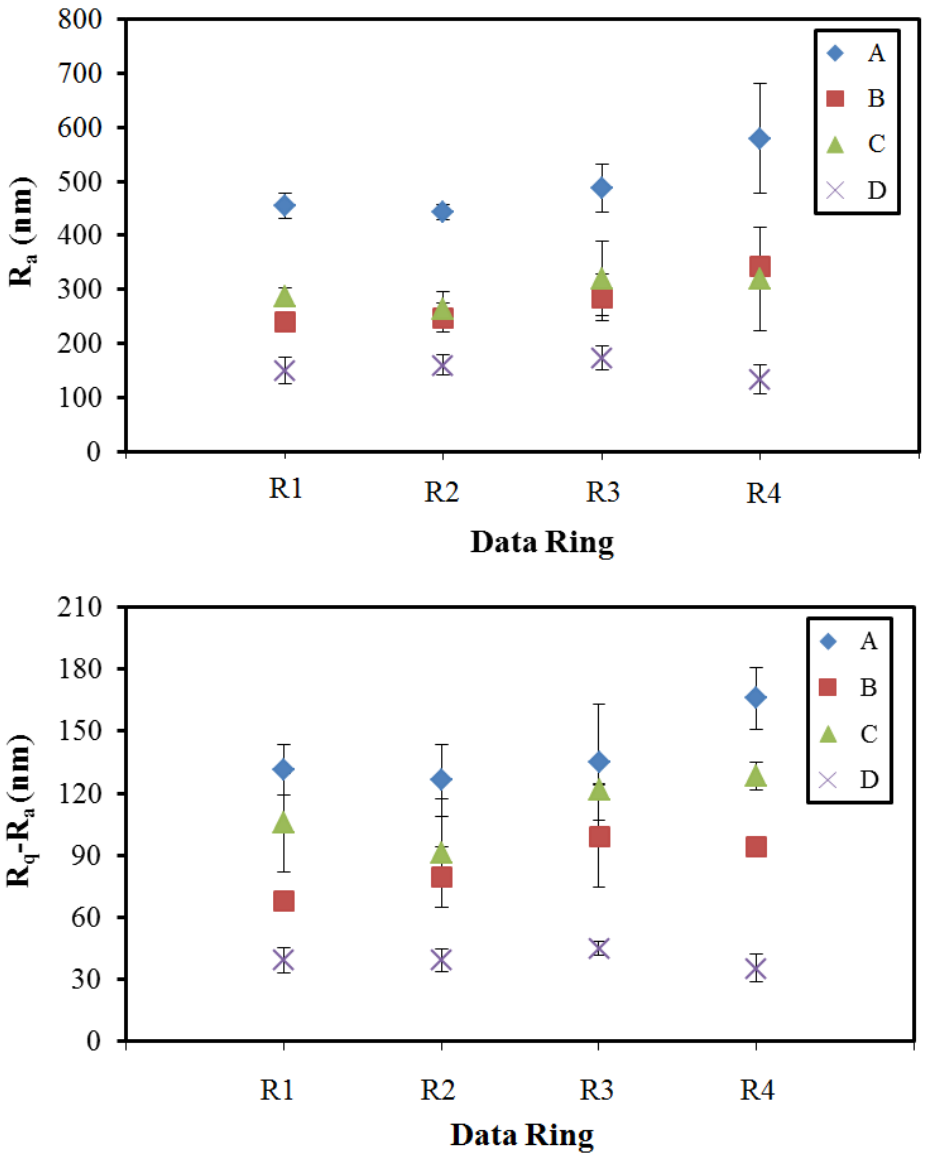

Fig.10 Surface roughness measurements of individual data rings taken for button B_1, R_a (top), R_q-R_a (bottom)

Furthermore, the higher Rq-Ra parameter points towards the lower surface uniformity across the surface of the button. It was also possible to see a great variation across the data points in comparison to inner rings such as R2. This trend was also observed in process B, where the

shape of the button did not allow a consistent hand polishing to be performed. The outcome of process C was directly related to the surface profile of process B, exhibiting similar behaviour. All data rings demonstrated an improving trend throughout the treatment procedure, with process D generating the best surface profile. However, R3 indicated a slight increase in the average roughness during EP. For all the processes the variation across the measured parameters increased towards the outer edges of the button. Average roughness was reduced for all data rings throughout the surface treatment. Process D exhibited fewer variations, highlighting the level of control over the process in comparison to other stages. The overall surface profile tends to be similar across the button surface once EP is performed.

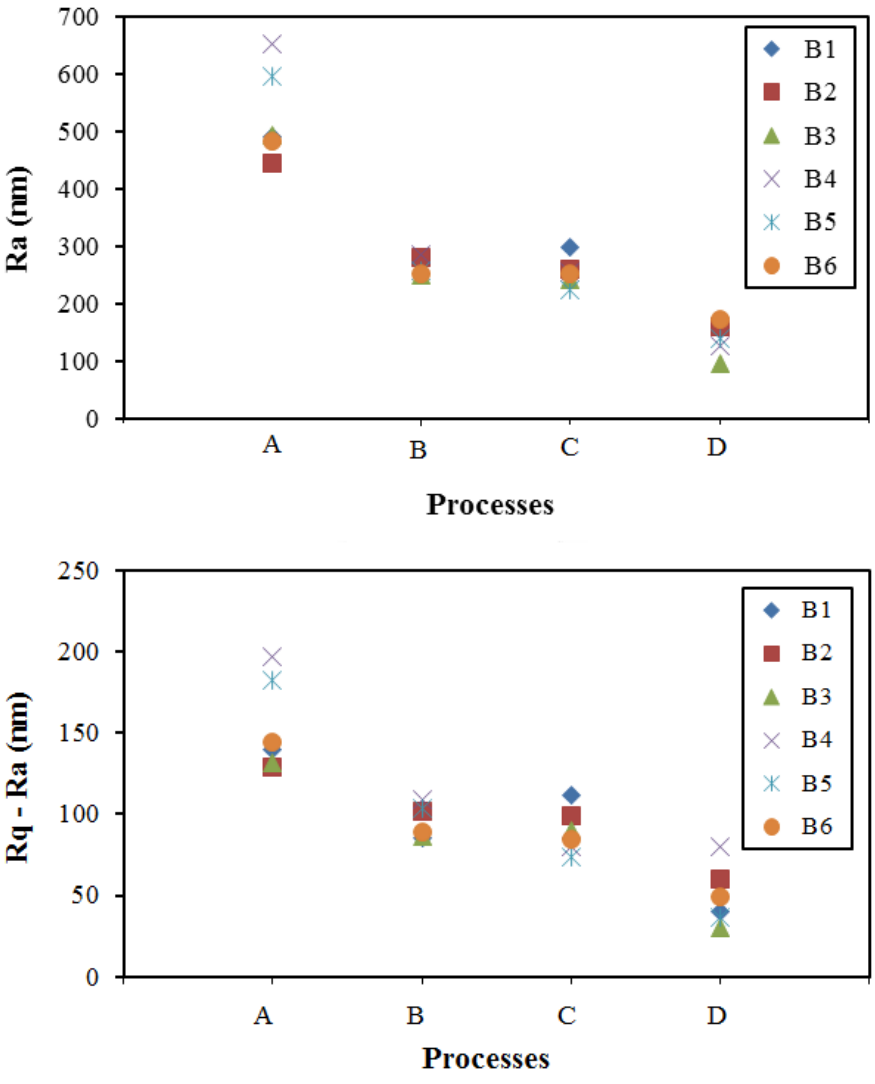

Fig. 11 Surface roughness measurements taken for buttons B1-B6, R_a (top), R_q-R_a (bottom)

To ensure the reliability of any findings, it was critical to investigate the reproducibility of the results. The procedure was repeated for six buttons and the findings are shown in Fig. 11.

Average roughness and surface uniformity parameters were calculated using the average of all data points. All buttons followed the improved trend in surface profile observed previously for B1. Process A showed a larger degree of variations across the six buttons.

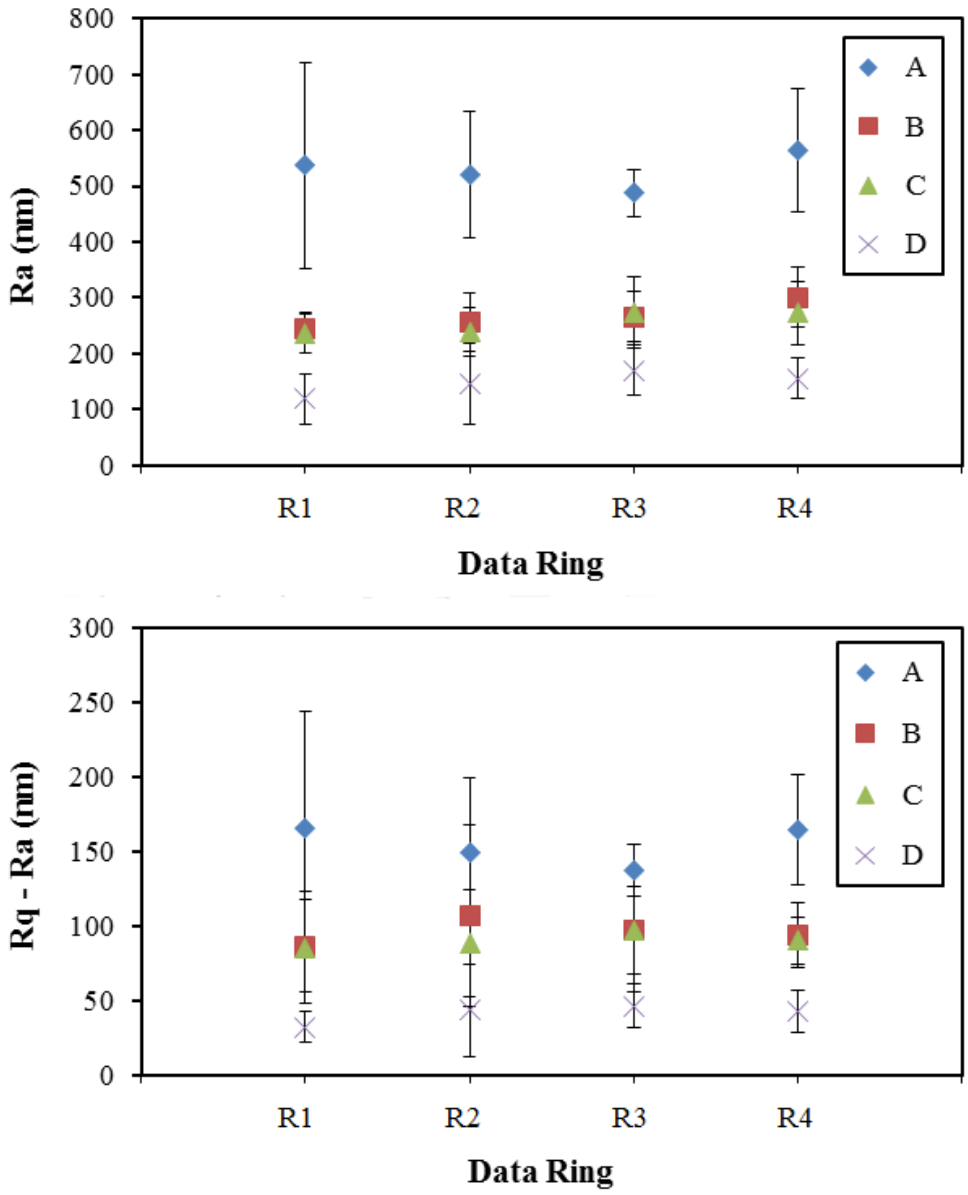

Fig. 12. Surface roughness measurements of individual data rings taken for buttons B_1 to B_6, R_a (top), R_q-R_a (bottom)

Individual data rings have also been investigated after each process, using the average of the data rings for all buttons. As shown in Fig. 12, surface quality was improved after each process with shrinking variations seen across all buttons.

Once again, surface measurements were taken for all the six button samples used in method two. Table 3 illustrates the surface roughness measurements taken for button B_7. As expected,

during processes A to D, the surface profile followed a similar trend previously seen for buttons B_1-B_6. Hence, the main focus was to investigate the alterations made to the surface quality while being electro plated. This stage of the surface treatment is referred to as process E.

Table 3: Average roughness (R_a) and root mean square (R_q) parameters for button B_7

Process	**A (as received)**	**B (had polished)**	**C (chemical etched)**	**D (EP)**	**E (EPL)**
R_a (nm)	434	240	228	95	62
R_q (nm)	564	284	315	126	79

Similar to the previous method, the change in the surface profile is visualised by a series of plots. Processes A to D are performed prior to electro plating in order to generate a subsurface that is suitable for process E. As shown below in Fig. 13, the surface quality of button B_7 behaves in an expected manner through processes A to D. It was evident that copper plating resulted in the reduction of the recorded average roughness of the surface. Furthermore, the reduction in the variation seen across the data points is a clear indication of the quality of the setup used to coat button B_7.

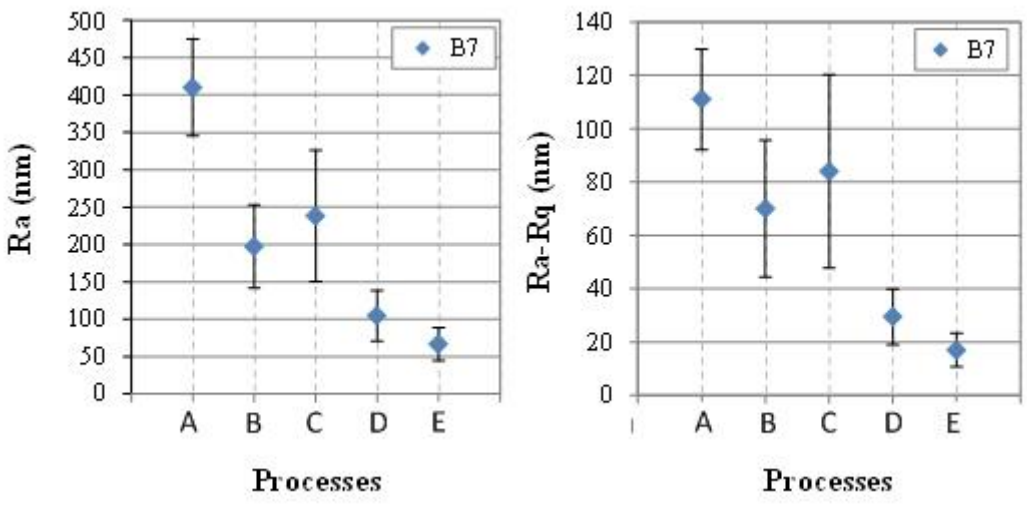

Fig. 13 Surface roughness measurements taken for button B_7, Ra (top); R_q-R_a (bottom)

Fig. 14 shows the improvements seen across individual data rings as button B_7 underwent surface treatment using method two. The surface quality exhibited by the inner data ring R1 was higher than the one observed on the outer edges of the button where R4 was situated. This was more evident for processes A and B in particular. The robust nature of the EP process enabled a high quality copper layer to be applied during plating process E. Further improvements in surface uniformity were observed once copper plating was carried out.

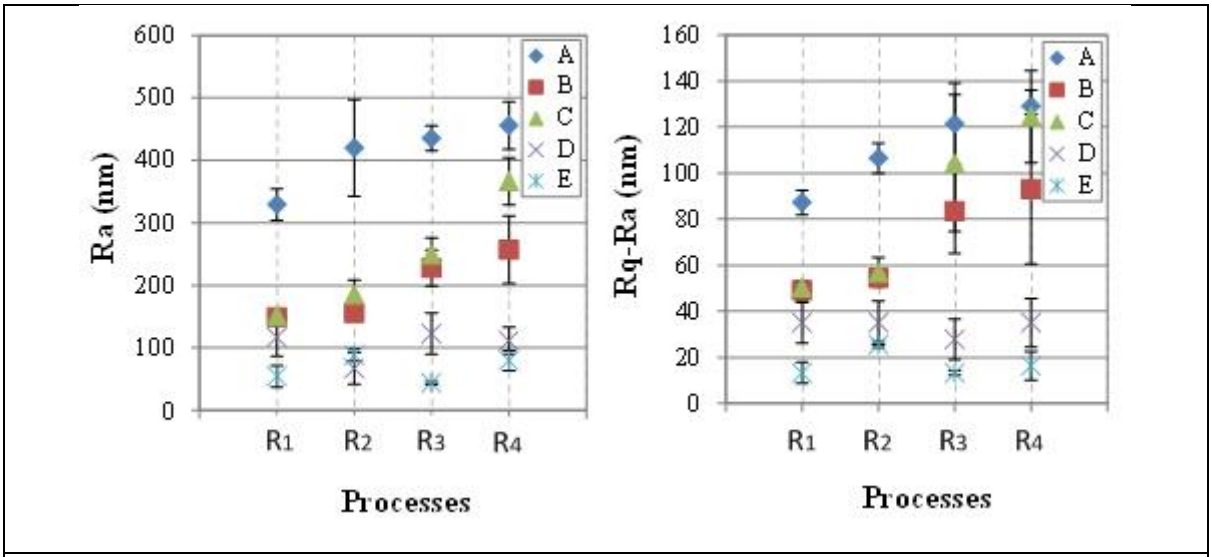

Fig. 14 Surface roughness measurements of individual data rings taken for button B_7, R_a (top), R_q-R_a (bottom)

Method 2 was repeated using six buttons in order to demonstrate the consistency of the findings. Fig. 15 illustrates the roughness measurements taken from button B7 to B12 for processes A to E. The findings were a strong indication of the reliability offered by the designed procedure to reproduce a similar surface quality for different buttons. All buttons displayed a higher surface quality alongside a much improved surface uniformity.

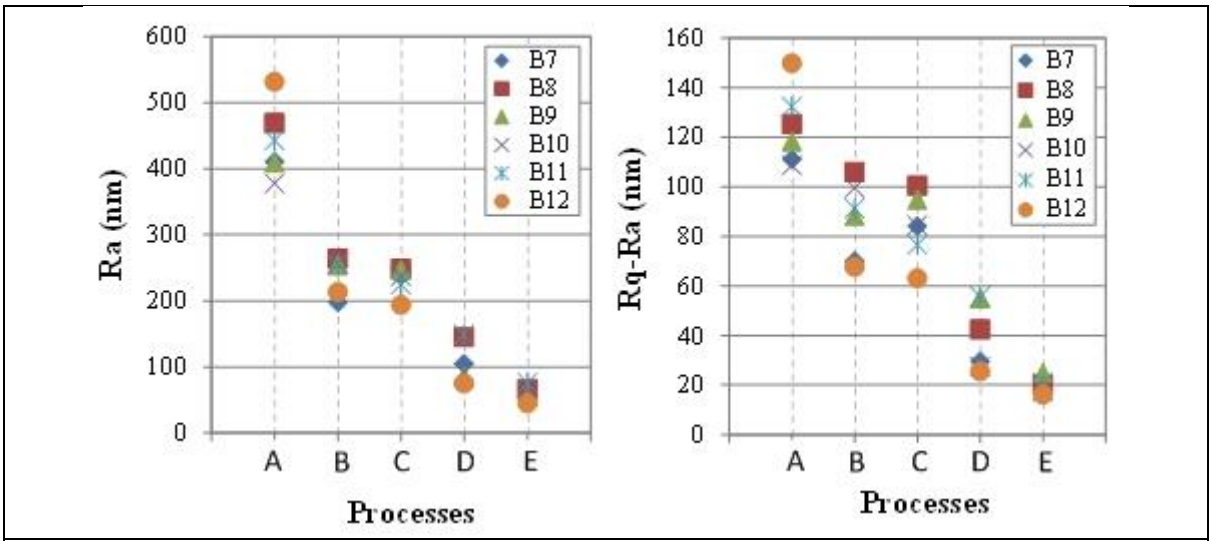

Fig. 15 Surface roughness measurements taken for buttons B7 to B12, R_a (top), R_q-R_a (bottom)

V. Conclusion

A series of buttons were manufactured and surface treated using two surface treatment methods each consisting of various steps. White light interferometer was employed in order to obtain roughness parameters and to characterise the surface quality.

The main technique employed in the first surface preparation method was electro polishing. Prior to EP, the surface of the button underwent two pre-treatment stages with the aim of removing damaged layers and chemical contaminations introduced during fabrication. The surface was initially hand polished using sand paper followed by acid chemical etching. Measurements showed how the surface was both chemically and physically altered at each step of surface preparation. Interferometry results showed that the treatment process was capable of significantly improve the surface quality observed across all button samples.

The second surface preparation technique concentrated on electroplating as the main surface treatment technique. The importance of the subsurface in obtaining a desirable surface finish after EPL was highlighted. It was shown that having a desirable subsurface allowed for the application of a stable and uniform copper layer on top of the existing treated surface.

In both approaches, all button samples showed extensive surface damage after fabrication. However, both processes were capable of achieving satisfactory results in lowering the surface roughness and improving uniformity. The investigations revealed the ability to produce a superior surface finish through EPL in comparison to EP. This opens new possibilities in the production of RF cavities by using new and improved surface treatment techniques.

Acknowledgment

One of the authors A. Z. wishes to thank the physics department of the Lancaster University for their help during the time the experimental part of this research was done.

References

1. M. Bogomilov, et al., *Neutrino Factory*. Phys. Rev. ST Accel. Beams, 17, 121002 (2014)
2. T. E. Edgecock, et al., *High Intensity Neutrino Oscillation Facilities in Europe* . Phys. Rev. ST Accel. Beams, 16, 021002 (2013)
3. D. Adams, et al., *Characterisation of the muon beams for the Muon Ionisation Cooling Experiment.* Eur. Phys. J. C (2013)73:2582
4. M. Bogomilov, et al., *The MICE Muon Beam on ISIS and the beam-line instrumentation of the Muon Ionization Cooling Experiment*. JINST, 7, P05009 (2012)
5. M. Bogomilov, et al., *Design and expected performance of the MICE demosntration of oonization cooling.* The MICE Collaboration, arXiv:1701.06403v2, 2017
6. http://www.mice.iit.edu/mta
7. http://www.map.fnal.gov/index.shtml
8. Yorun, Y., et al. The MUCOOL Test Area and RF Program in IPAC 10. 2010. Kyoto, Japan
9. Huang,D., et al., 805 MHz cavity button test – Cavity material study at MTA, FNAL, 2008, Fermilab. P.18.
10. R.B Palmer, et al., *RF breakdown with external magnetic fields in 201 and 805 MHz cavities.* Phys. Rev. ST Accel. Beams, 12, 031002 (2009)
11. Gadelmawla, E.S., et al., *Roughness parameters.* Journal of Materials Processing Technology, 2002. 123(1): p. 133-145.
12. J. Norem, et al., In Proceedings of 2005 Particle Accelerator Conference. Knoxville, Tennessee, USA (2005) p.2104
13. Y. Torun, et al., In Proceedings of IPAC'10, Kyoto, Japan (2010) p. 3780.
14. C. Johnstone, A. Bross, and I. Rakhno. In Proceedings of 2005 Particle Accelerator Conference. Knoxville, Tennessee, USA (2005) p.3482
15. T. Luo, et al., In Proceedings of IPAC12. New Orleans, Luisinia, USA (2012) p. 3398
16. D. Huang, et al., In Proceedings of PAC09. Vancouver, BC, Canada (2009) p.888

17. D. Li, et al., In Proceedings of the 2003 *Particle Accelerator Conference*. Portland, Oregon, USA (2003) p.1246
18. J. Norem, et al., In Proceedings of Particle Accelerator Conference, Albuquerque, New Mexico, USA *(*2007) p.2239.
19. A. Zarrebini-Esfahani, et al., In Proceedings of PAC09, Vancouver, BC, Canada (2009) p.1982.
20. A. Zarrebini-Esfahani, et al., In Proceedings of IPAC'10, Kyoto, Japan (2010) p. 3004
21. V. A. Dolgashev, et al., In Proceedings of 2005 Particle Accelerator Conference. Knoxville, Tennessee, USA (2005) p. 595
22. Smiths Metal Centres Ltd. *Material Guide* 2007 [cited 2007; Available from: http://www.smithmetal.com/.
23. M. Bertucci, et al., Review of Scientific Instruments 87, 013103 (2016)
24. D. Stratakis, Juan C. Gallardo, and Robert B. Palmer, Nucl. Instrum. Methods Phys. Res., Sect. A, 643 (2011) 1-5.
25. S. Ahmad, J. Mammosser, Review of Scientific Instruments 86, 073303 (2015)
26. C.F. Eyring, S.S. Mackeown, and R.A. Millikan, *Field Currents from Points.* Physical Review, 1928. 31(5): p. 900-909.